Charge transfer from neutral perfluorocarbons to various cations: long-range versus short-range reaction mechanisms

G.K. Jarvis[a], R.A. Kennedy[b], C.A. Mayhew[a],*, R.P. Tuckett[b]

[a]*School of Physics and Astronomy,* [b]*School of Chemistry, University of Birmingham, Edgbaston, Birmingham B15 2TT, UK*

Abstract

The bimolecular reactions of the high recombination energy cations Ar^+, F^+, and Ne^+ with four fully saturated (CF_4, C_2F_6, C_3F_8, and $n\text{-}C_4F_{10}$) and three unsaturated (C_2F_4, C_3F_6, and $2\text{-}C_4F_8$) perfluorocarbons (PFCs) are reported. The cation branching ratios obtained from these reactions, and from the reactions with O_2^+, H_2O^+, N_2O^+, O^+, CO_2^+, CO^+, N^+, and N_2^+ [reported by us, Jarvis et al., J. Phys. Chem. 100 (1996) 17166], are compared with those determined from the threshold photoelectron–photoion coincidence spectra of the PFCs at the recombination energies of the reagent cations. This comparison provides information that helps to interpret the dynamics of charge transfer, and whether it occurs via a long-range or a short-range mechanism. Energy resonance and good Franck-Condon factors connecting the ground electronic state of a reactant neutral molecule to one of its ionic states, at the recombination energy of the reagent cation, are generally considered to be sufficient criteria for long-range charge transfer to occur. However, the results from this study imply that good Franck-Condon factors are not critical in determining the efficiency of a long-range charge transfer. Instead, the results suggest that, in addition to the requirement for energy resonance, the electron taking part in the charge-transfer process must be removed from a molecular orbital which is unshielded from the approaching reagent cation. This enables the cation to exert an influence on the electron at large impact parameters. (Int J Mass Spectrom 202 (2000) 323–343) © 2000 Elsevier Science B.V.

*Keywords:* SIFT; Charge transfer; Perfluorocarbons; TPEPICO

1. Introduction

Charge transfer between neutral molecules and cations is an important class of ion–molecule reactions, being significant in terrestrial, industrial, and astrophysical plasmas. In view of the apparent simplicity of charge transfer it should be possible to predict both the reaction rate coefficient and the reactant products. Success in this endeavour would represent a significant contribution to the provision of input information for the modeling of discharge plasmas, and to the identification of the cations responsible for plasma/surface interactions. The experimental tools to be employed are studies of the rate coefficients and products of ion–molecule reactions, allied to investigations of the energy selective fragmentation of molecular cations. In this article, we present data on a number of small perfluorocarbons (C_nF_{2n} or C_nF_{2n+2}, $n \leq 4$), and review some past investigations of their ion–molecule reactions.

Charge transfer (involving the transfer of an electron from the neutral reactant species to the reagent cation) can be nondissociative (1) or dissociative (2):

$$A^+ + BC \rightarrow A + (BC^+)^* \rightarrow A + BC^+ \qquad (1)$$

$$\rightarrow A + B^+ + C \qquad (2)$$
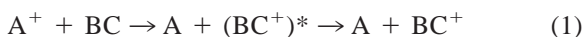
More complex reactions involving the transfer of atoms (3) can also occur in competition with or instead of charge transfer:

$$A^+ + BC \rightarrow AC + B^+ \qquad (3)$$

Since most experimental methods only allow the product cations to be identified, without further information it is not always possible to ascertain whether the overall reaction is charge transfer.

Important findings from past experimental studies of charge-transfer reactions [1–11] between thermalised cations and molecules include the following. (1) Charge-transfer reactions are usually fast, with experimentally observed reaction rate coefficients, k_{obs}, not significantly different from the values, k_c, predicted by ion–molecule capture theories. (2) There are no charge-transfer reactions for which it has been possible to demonstrate conclusively that the rate coefficient exceeds that predicted by capture theories. (3) For reactions in which the rate coefficient is less than given by capture theories, an examination of the photoelectron spectrum of the neutral molecule (BC) at the recombination energy of the cation (A^+), which may be atomic or molecular, frequently reveals a low photoionisation efficiency at this energy. (4) The reaction rate coefficients do not closely parallel the intensity profiles in the photoelectron spectra. Variations in the rate coefficients with recombination energy are generally less marked than the changes in the photoelectron signal as a function of ionisation energy. Further, at energies where the photoelectron signal has fallen to a low level, charge-transfer can still proceed at a large fraction of the maximum (capture) rate. (5) Energy resonance between the recombination energy of A^+ and an ionisation energy of BC is important for an efficient reaction. This is most apparent in studies on simple molecules. In more complicated systems, the high density of vibronic states (including those arising from dissociation) en-

sures that energy resonance can be satisfied, and that the extent of variations in the rate coefficient with recombination energy of the cation is limited.

The favoured model within which to interpret these observations is that of a "long-range" charge-transfer mechanism. The cation and neutral approach under the influence of their mutual charge-induced dipole attraction, until at some critical separation the potential energy curves for A^+–BC and A–BC^+ cross. Assuming that the potential can be expressed purely in terms of the charge-induced dipole interaction, the critical separation, R_{CT}, is given by

$$R_{CT} = \left\{ \frac{\alpha(BC) - \alpha(A)}{RE(A^+) - IE(BC)} \frac{e^2}{8\pi\varepsilon_0} \right\}^{1/4} \qquad (4)$$

where $RE(A^+)$ is the recombination energy of the reagent cation, $IE(BC)$ is the ionisation energy of the reactant neutral to a vibronic level in BC^+, $\alpha(BC)$ is the polarisability volume of the reactant neutral, $\alpha(A)$ is the polarisability volume of the product neutral, e is the electron charge, and ε_0 is the permittivity of free space. Eq. (4) illustrates that there is a strong energy resonance criterion between the recombination energy of the cation and the ionisation energy of the molecule. Unless the difference between $RE(A^+)$ and $IE(BC)$ is very small, the separation at which the two curves cross is short. For example, in the case of the reaction between Ar^+ and CF_4, the difference between the recombination energy of Ar^+ and the ionisation onset potential of CF_4 is 0.22 eV. (We define the ionisation onset potential as the minimum photon energy required in photoionisation measurements to produce an observable ion and/or electron signal. It represents an upper limit to the adiabatic ionisation potential.) Eq. (4) then gives $R_{CT} = 2.9$ Å, and this is better described as an intimate interaction than a long-range electron jump, and the potential will not be well expressed by charge-induced dipole term alone. If we consider the reaction between Ar^+ and CF_4 further, the difference between $RE(Ar^+)$ and $IE(CF_4)$ must be less than 0.025 eV for the curve crossing to occur at $R_{CT} \geq 5$ Å. Thus, for a charge-transfer reaction to occur at long range through an electron jump at a curve crossing, it will generally be

necessary to produce a vibronically excited product cation.

In the long-range model, it is expected that the electron jump will occur on a time scale which is short compared to that for nuclear motion, and that the potential energy curves of the reactant neutral molecule are not significantly distorted by the approaching cation. This has been taken to imply that the Franck-Condon principle will be important in assessing the efficiency of charge transfer. For the coordinates orthogonal to the relative approach of the two reactants, there must be good overlap of the vibrational wave functions of the neutral reactant, BC, with an ionic state, BC^+, and, for a molecular reagent cation, of A^+ with A. When this is combined with the energy resonance criterion, it is seen that the photoelectron spectrum of the reactant neutral molecule should provide a guide as to when long-range charge transfer may be efficient. When the vertical recombination energy of the cation matches the ionisation energy of a region of the photoelectron spectrum with a strong signal, then both the energy resonance and Franck-Condon principle criteria are satisfied, and long-range charge transfer should be efficient.
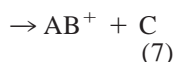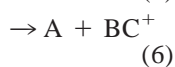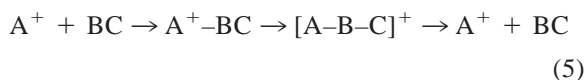
It should be noted that the simple long-range model does not take into account possible differences in the intrinsic probability for removal of an electron from a particular orbital in a charge-transfer reaction. These may be different from the ionisation probabilities for photon impact, which are revealed in the photoelectron spectrum of the molecule. A further major difficulty with the long-range picture of charge-transfer reactions, is that there are no examples in which it has been conclusively shown that $k_{obs} > k_c$, as might be anticipated for a long-range reaction in which a large capture cross section is expected because of a large R_{CT} [Eq. (4)].

Owing to the nature of the capture models it is not possible to give a unique separation at which charge transfer takes place. However, if the capture rate coefficient, k_c, for $Ar^+ + CF_4$ is mapped onto a hard sphere model, the distance of approach corresponding to capture is 7.7 Å. As this critical impact parameter is large, an electron jump could occur at distances less than this value without strongly perturbing the poten-

tial energy surfaces. In all cases, the observed rate coefficients suggest that capture is an essential first step before charge transfer occurs. If the charge transfer leads to dissociation of the product cation, reaction (2), then the capture complex will be destroyed, preventing any possibility of intimate interactions within the complex. Evidence for intimate interactions in ion–molecule reactions can be sought in a number of ways. If cation products are observed in which atoms have been transferred between the reactants, then intimate contact has occurred for some encounters.

As mentioned above, the long-range model predicts a strong correlation between the photoelectron spectrum of the neutral molecule and the rate of charge transfer as a function of reagent cation recombination energy. Some relaxation may be permitted in the sense that the reaction efficiency (k_{obs}/k_c) measures the probability that reaction occurs during an encounter of a cation with a molecule, rather than the photoionisation cross section. Quite a low value for the latter may still be sufficient to give a high probability for charge transfer during an encounter. There remain many examples in which substantial extensions to the Franck-Condon envelope of a photoelectron band, outside those that could be anticipated from the argument above, have been reported. If reaction cannot occur at long range, due to the lack of an energy resonance, then the reactants will move closer. Two types of behaviour are then possible. The first possibility is that the reactants retain their molecular identities, but their mutual interactions disturb their respective potential energy surfaces, so modifying the vibrational wave functions and associated Franck-Condon factors. Eventually a separation may be reached where there is a potential energy curve crossing for a (distorted) product vibronic level, and for which the distorted Franck-Condon factors are sufficiently large to lead to efficient (short-range) charge transfer. This may account for efficient charge-transfer reactions occurring for cations with recombination energies close to, but outside the bands of the photoelectron spectrum. For some reactions, the energy available may not produce a sufficient distortion of the potential energy surfaces to result in efficient

charge transfer, and the reaction probability will be small. Simple model calculations on the interaction of a point charge with N_2 and CO, indicate that for these, rather rigid molecules, a very close approach (within 1.5 Å) of the cation to the neutral molecule is required to produce a significant distortion of the Franck-Condon factors. The second possibility is that as the reactants approach they lose their integrity, through the formation of a new chemical bond. The intermediate formed in this way will subsequently fragment:

$$A^+ + BC \rightarrow A^+\text{–}BC \rightarrow [A\text{–}B\text{–}C]^+ \rightarrow A^+ + BC \tag{5}$$

$$\rightarrow A + BC^+ \tag{6}$$

$$\rightarrow AB^+ + C \tag{7}$$

Three pathways can be distinguished: Eq. (5) is the regeneration of the reactants, Eq. (6) is the release of the parent product cation and/or fragment cations (charge transfer by means of a chemically bound intermediate), and Eq. (7) is the release of product cations in which the new bond formed in the intermediate is preserved, and bonds associated with the reactant neutral are broken (an intimate reaction). This second short-range mechanism does not involve a curve crossing, so that the reaction efficiency will not depend on energy resonance and Franck-Condon factors. This mechanism can lead to charge-transfer reactions with rate coefficients equal or close to the capture rate coefficient for any pair of reactant cation and neutral. Its occurrence may be recognised through the observation of fast reactions when the recombination energy of the cation is far from any band in the photoelectron spectrum of the neutral reactant molecule, and through detection of cation products, which result from the transfer of atoms between the reactants. The existence of an intermediate with a variety of different fragmentation pathways is a key feature of this mechanism. Consideration of the energetics and possibilities for bond formation indicates that rare gas cations are unlikely to react by means of this mechanism, but that unsaturated molecules will be good candidates, through intermediate formation by electrophilic attack.

The long-range mechanism, through its energy resonance and Franck-Condon criteria, leads naturally to specific predictions about the vibronic state of the initially produced cation. These predictions have been tested experimentally in a few cases, through observations that are sensitive to the energy content of the cation product. Thus in the case of the reactions of F^+ with NO and O_2 (both are efficient reactions, $k_{obs}/k_c \approx 1$), production of vibronically excited cations was demonstrated through their subsequent reactions with Ar [10]. For many polyatomic parent cations, the ions dissociate rapidly upon formation, and the relative yields of different fragment cations are characteristic of the initial vibronic state of the cation. The fragmentation patterns of energy-selected cations produced by photoionisation can be determined through the observation of threshold photoelectron–photoion coincidences (TPEPICO). These data can be compared with the branching ratios observed from ion-molecule reactions. A cation formed by long-range charge transfer may be expected to display the same fragmentation pattern as one formed by photoionisation, using a photon energy equal to the recombination energy of the reagent cation, because the product neutral will be a distant spectator to the fragmentation. If the reaction occurs at short range, the presence of the product neutral will distort the product cation, and so lead to a modification of the product fragment cation branching ratios, compared to those predicted on the basis of TPEPICO data.

The use of photoionisation coincidence data, to assist in the interpretation of the results of studies of charge-transfer reactions, was explored in a recent investigation of the charge-transfer reactions of CCl_4 and SF_6 by Williams et al. [11]. Little evidence was found for differences in branching ratio patterns between photoionisation and charge-transfer reactions. Even for cases where the reaction rate coefficient is much below the capture rate coefficient, there are no obvious differences. However, the number of systems to which this technique has been applied is very small, and it may yet yield data that will assist in the elucidation of the mechanisms by which charge-transfer reactions occur.

Most past studies of charge-transfer reactions have

tended to look at the reactions of a specific cation with a range of different molecules. In this article we have chosen to study a series of related molecules, with cations spanning a range of recombination energies. The molecules selected are small saturated and unsaturated perfluorocarbons. These compounds are constituents of gas mixtures used in a number of plasma processing applications. To explore the interpretation of the data-reaction rate coefficients and cation product branching ratios-we have also recorded threshold photoelectron spectra and TPEPICO data for each of the molecules [12,13]. This work builds upon an earlier study [9] of the reactions of C_2F_6, C_3F_8, n-C_4F_{10}, C_2F_4, C_3F_6, and 2-C_4F_8 with a range of important atmospheric cations (H_3O^+, NO^+, O_2^+, H_2O^+, N_2O^+, O^+, CO_2^+, CO^+, N^+, and N_2^+). The recombination energies of these cations vary from 6.37 to 15.58 eV. Our earlier study suggested that, for the majority of reactions, long-range charge transfer does not take place to any significant amount, and short-range processes, including charge-transfer channels, dominate. Here we extend the earlier cation-PFC study by reporting the bimolecular rate coefficients and cation products for the reactions of higher-energy recombination atomic cations Ar^+, F^+, and Ne^+ with the above PFCs.

The reactions of Ar^+, F^+, and Ne^+ with CF_4 are also presented here. We did not investigate cation reactions with CF_4 in our previous study, because the ionisation onset potential of CF_4 (15.54 eV) is greater than the recombination energies of the cations used in that study. These cations can therefore only react chemically, if at all, with CF_4. The exception is N_2^+, whose adiabatic recombination energy (15.58 eV) is close to the ionisation onset potential of CF_4. Therefore, for completeness, the reaction of N_2^+ with CF_4 is reported in this article. The three reagent cations of this new study have recombination energies higher than the ionisation onset potential of CF_4, namely; 15.76 eV for Ar^+, 17.42 eV for F^+, and 21.56 eV for Ne^+. Comparisons of the reactions of N_2^+ and Ar^+ with the PFCs are particularly interesting in that, whilst their recombination energies are similar, N_2^+ may chemically react with the PFCs whereas Ar^+ cannot.

Of the new reactions investigated and reported in this present study, i.e. those involving Ar^+, F^+, and Ne^+, only that of Ar^+ with CF_4 [14–16] and C_2F_6 and C_2F_4 [17] have been previously published. Chau and Bowers [14] have also reported the reaction of N_2^+ with CF_4, which they investigated by use of an ion cyclotron resonance technique. The kinetic results and cation product branching ratios (when given) from these other studies are in good agreement with those presented here.

2. Experimental

The experimental procedure for the acquisition of the TPEPICO data has been presented in detail previously [18,19]. In brief, the apparatus utilised monochromatised synchrotron radiation, which ionises molecules injected effusively into an interaction region. Ions and electrons produced were extracted in opposite directions by an electric field strength of 20 V cm^{-1}. Threshold electrons passed through a steradiancy-type analyser followed by a 127° postanalyser before being detected by a channel electron multiplier. Ions were accelerated through a linear time-of-flight mass spectrometer incorporating space focusing. The arrival time of the ions were then recorded relative to the threshold electrons to produce fragmentation patterns of state-selected molecular ions. All spectra were recorded with an optical resolution of 0.4 nm.

A selected ion flow tube (SIFT) was used to measure the reaction rate coefficients and cation products of the bimolecular reactions. The SIFT apparatus, experimental technique, and analysis of data have been extensively reviewed [20]. Only the essential information is provided here. Details of the production of the reagent cations O_2^+, H_2O^+, N_2O^+, O^+, CO_2^+, CO^+, N^+, and N_2^+ have been described in the earlier paper [9]. Ar^+, F^+, and Ne^+, were generated in an ion source containing either Ar, CF_4, or Ne, respectively. The mass selected reagent cations were injected via a Venturi inlet into a fast flowing (~150 Torr L s^{-1}) He (99.997% purity) buffer gas maintained at 300 K and ~0.5 Torr. The cations were thus

convected by the helium down the flow tube. Measured quantities of reactant gases were introduced into the carrier gas/cation stream downstream of the cation inlet through a ring port positioned at a known distance from a Faraday plate at the end of the flow tube.

A small percentage of the parent and product cations were focused through an orifice (~1 mm) in the Faraday plate, mass analysed by a quadrupole mass filter and detected by a channel electron multiplier. By correlating the decrease of the parent cation count rate and the increase in the product cation count rates to the flow rate of the neutral reactant molecule, the rate coefficient and cation product distributions were obtained, respectively. The accuracy of the measured rate coefficients is $\pm20\%$. The product cation branching ratios were determined by plotting product percentages against the flow rate of the reactant neutral and extrapolating to zero flow. This procedure allows for any secondary reactions in the flow tube to be accounted for. Mass discrimination of the detection system was taken into account in the usual way [21]. Even with this approach, a number of contaminant cations, produced in the flow tube (see the following), resulted in some problems in determining accurate branching ratios. We estimate that the uncertainty in any branching ratio is $\pm10\%$.

For this study, the cations were generated in a high-pressure ion source. The Ar^+ and Ne^+ cations therefore underwent multiple collisions with the parent atom and should have emerged from the source in their ground electronic state, $^2P_{3/2}$. Even if this were not the case, the energy separation between the $^2P_{3/2}$ and $^2P_{1/2}$ states is only 0.10 eV for Ne^+ and 0.18 eV for Ar^+, and therefore differences in reactivities between the two spin-orbit states are not expected. Certainly, none were observed. The ground state of F^+ is a closely spaced triplet with recombination energies of 17.42 eV ($^3P_2$), 17.47 eV ($^3P_1$), and 17.48 eV ($^3P_0$). Thus, for this cation, the energy splitting is sufficiently small that the states should have been maintained in a Boltzmann distribution through collisions with the helium buffer gas. Due to the smallness of these energy splittings, no differences in the reactivity of the F^+ cation in its various

spin-orbit states is to be expected. For the other reagent cations of the earlier study, a significant fraction of the N_2^+ and O_2^+ cations were vibrationally excited [9]. By studying the reaction of N_2^+ with Ar, it was found that N_2^+ ($v = 1$) amounted to about 40% of the total reagent cation signal. For the O_2^+ cation, reactions with Xe and SO_2 indicated that approximately 20% of the O_2^+ was present in the $v = 1$ and 2 levels, and the lack of reaction with H_2O showed that the $v \geq 3$ levels were unpopulated.

When either Ar^+ or F^+ cations were injected into the flow tube, trace H_2O in the flow tube and carrier gas led to the formation of H_2O^+, with a signal level of about 3% of the reagent cation signal. Reactions of Ne^+ with the trace H_2O led to impurity cation signals of OH^+ and H_2O^+ in the flow tube at a level of about 5% and 3%, respectively, of that of Ne^+. In addition $HeNe^+$ cations were formed in the flow tube from termolecular reactions of Ne^+ with the helium buffer gas:

$$Ne^+ + 2He \rightarrow HeNe^+ + He \qquad (8)$$
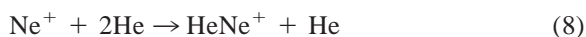
This led to a $HeNe^+$ signal of about 2%–3% of the Ne^+ signal. The reactions of H_2O^+ with the PFCs were easily accounted for by using the results from our previous study [9]. However, in the Ne^+ study, no allowance has been made in the product cation branching ratios for the reactions of $HeNe^+$ and OH^+ with the PFCs.

The reactant gases were obtained commercially with CF_4, C_2F_4, C_2F_6, and C_3F_6 having stated purities of $>99\%$, and $2\text{-}C_4F_8$, C_3F_8, and $n\text{-}C_4F_{10}$ having stated purities of 97%. They were used without further purification. The sample of $2\text{-}C_4F_8$ contained a mixture of the cis and trans isomers.

3. Results

The reaction rate coefficients and product cation information for the reactions of O_2^+, H_2O^+, N_2O^+, O^+, CO_2^+, CO^+, N^+, and N_2^+ with C_2F_6, C_3F_8, $n\text{-}C_4F_{10}$, C_2F_4, C_3F_6, and $2\text{-}C_4F_8$ have been published [9]. The measured rate coefficients, k_{obs}, the product cations and their branching percentages for the reac-

Table 1

The measured 300 K reaction rate coefficients (in units of 10^{-9} cm^3 molecule^{-1} s^{-1}), k_{obs}, and cation product branching ratios (percentage) for the reactions of the saturated PFCs CF$_4$, C$_2$F$_6$, C$_3$F$_8$, and n-C$_4$F$_{10}$ [ionisation onset potentials (IP) in eV and polarizabilities are given in parentheses] with Ar$^+$, F$^+$, and Ne$^+$ [recombination energies (RE) in eV are given in parentheses]. The collisional rate coefficients, k_c, calculated using Langevin theory [22] are also presented (see the text for more details). The estimated uncertainty in the measured rate coefficients is $\pm 20\%$ and is $\pm 10\%$ for the cation branching ratios

	PFC (IP/eV)	CF$_4$ (15.54) ($\alpha = 3.83$ Å^3)			C$_2$F$_6$ (13.4) ($\alpha = 6.82$ Å^3)			C$_3$F$_8$ (13.0)[a] ($\alpha_{eff} = 6.7 \pm 0.7$ Å^3)[b]			n-C$_4$F$_{10}$ (12.6)[a] ($\alpha_{eff} = 11.0 \pm 0.5$ Å^3)[b]		
		k_{obs}	k_c	Ionic products (%)	k_{obs}	k_c	Ionic products (%)	k_{obs}	k_c	Ionic products (%)	k_{obs}	k_c	Ionic products (%)
	Ar$^+$ (15.76)	0.81	0.88	CF$_3^+$ (100)	0.98	1.1	CF$_3^+$ (19) C$_2$F$_5^+$ (81)	1.2	1.1	CF$_3^+$ (26) C$_2$F$_4^+$ (4) C$_2$F$_5^+$ (12) C$_3$F$_7^+$ (58)	1.1	1.3	CF$_3^+$ (21) C$_2$F$_4^+$ (3) C$_2$F$_5^+$ (21) C$_3$F$_6^+$ (1) C$_3$F$_7^+$ (2) C$_4$F$_9^+$ (52)
Ion (RE/eV)	F$^+$ (17.42)	1.1	1.2	CF$_3^+$ (100)	1.4	1.5	CF$_3^+$ (13) C$_2$F$_5^+$ (87)	1.3	1.5	CF$_3^+$ (70) C$_2$F$_4^+$ (2) C$_2$F$_5^+$ (2) C$_3$F$_7^+$ (26)	1.6	1.8	CF$_3^+$ (78) C$_2$F$_5^+$ (7) C$_3$F$_5^+$ (15)
	Ne$^+$ [c] (21.56)	0.06	1.1	CF$_3^+$ (100)	1.6	1.5	CF$^+$ (3) CF$_3^+$ (95) C$_2$F$_5^+$ (2)	1.5	1.4	CF$^+$ (3) CF$_3^+$ (87) C$_2$F$_4^+$ (3) C$_2$F$_5^+$ (7)	1.7	1.8	CF$_3^+$ (78) C$_2$F$_4^+$ (2) C$_2$F$_5^+$ (18) C$_3$F$_5^+$ (2)

[a] The ionisation onset potentials of C$_3$F$_8$ and n-C$_4$F$_{10}$ have been taken from [12].
[b] These polarizabilities (in units of Å^3 = 10^{-30} m^3) have been taken from values obtained in our previous study [9].
[c] Ion branching ratios include products resulting from the reactions of ions formed in the flow tube; OH$^+$ (5%) and HeNe$^+$ (3%).

tions of Ar$^+$, F$^+$, and Ne$^+$ with the saturated PFCs (CF$_4$, C$_2$F$_6$, C$_3$F$_8$, and n-C$_4$F$_{10}$) are presented in Table 1 and with the unsaturated PFCs (C$_2$F$_4$, C$_3$F$_6$, and 2-C$_4$F$_8$) in Table 2. Also shown in Tables 1 and 2 are the calculated collisional rate coefficients, k_c. For the nonpolar molecules CF$_4$, C$_2$F$_4$, and C$_2$F$_6$, k_c was determined using the Langevin equation [22]. For the polar molecules, polarizabilities and dipole moments are not listed in the literature. We have therefore used "effective" polarizabilities, which were determined in the previous study by examining the dependence of the rate coefficient of a polar molecule on the reduced mass of the colliding molecules at a fixed temperature [9]. For convenience, the data on the reaction of N$_2^+$ with CF$_4$, which we also investigated in this study, are not included in Table 1. This reaction proceeded at $k_{obs} = 1.1 \times 10^{-9}$ cm^3 molecule^{-1} s^{-1} ($k_c = 1.0 \times 10^{-9}$ cm^3 molecule^{-1} s^{-1}) producing CF$_3^+$ as the only cation product.

Threshold photoelectron spectra (TPES) for each of the saturated and unsaturated PFCs of this study are presented in Figs. 1 and 2, respectively. The recombination energies of the various reagent cations are marked in Figs. 1 and 2. These figures are useful for determining the presence of any resonance (ionic) states of the reactant molecule accessible at the recombination energy of the reagent cation. They are particularly useful when no PES of the reactant PFC is available in the literature. It should be noted that nonresonant photoelectron techniques are more suited to determine where the resonances occur, because they should be free of autoionisation effects. However, the TPES recorded by us agree well with the positions of resonances recorded by PES (CF$_4$ [23], C$_2$F$_6$ [24], C$_2$F$_4$ [25], C$_3$F$_6$ [26], and 2-C$_4$F$_8$ [27]), although some differences are observed. Certainly, in comparison to the PES, more structure is observed in the TPES, presumably resulting from autoionisation ef-

Table 2

The measured 300 K reaction rate coefficients (in units of 10^{-9} cm^3 molecule^{-1} s^{-1}), k_{obs}, and cation product branching ratios (percentage) for the reactions of the unsaturated PFCs C_2F_4, C_3F_6, and 2-C_4F_8 [ionisation onset potentials (IP) in eV and polarizabilities are given in parentheses] with Ar$^+$, F$^+$, and Ne$^+$ [recombination energies (RE) in eV are given in parentheses]. The collisional rate coefficients, k_c, calculated using Langevin theory [22] are also presented (see the text for more details). The estimated uncertainty in the measured rate coefficients is $\pm 20\%$ and is $\pm 10\%$ for the cation branching ratios

	PFC (IP/eV)	C_2F_4 (10.12) ($\alpha = 4.2$ Å^3)			C_3F_6 (10.6) ($\alpha_{eff} = 9.7 \pm 0.9$ Å^3)ᵃ			2-C_4F_8 (11.1) ($\alpha_{eff} = 13.7 \pm 0.8$ Å^3)ᵃ		
		k_{obs}	k_c	Ionic products (%)	k_{obs}	k_c	Ionic products (%)	k_{obs}	k_c	Ionic products (%)
Ion (RE/eV)	Ar$^+$ (15.76)	0.88	0.88	CF^+ (17) CF_2^+ (28) CF_3^+ (27) $C_2F_3^+$ (24) $C_2F_4^+$ (4)	1.3	1.3	CF_3^+ (2) $C_2F_4^+$ (18) $C_3F_5^+$ (80)	1.1	1.3	CF_3^+ (3) $C_3F_5^+$ (8) $C_3F_6^+$ (13) $C_4F_7^+$ (76)
	F$^+$ (17.42)	1.1	1.1	CF_2^+ (38) CF_3^+ (40) $C_2F_4^+$ (22)	1.7	1.8	CF_3^+ (11) $C_2F_4^+$ (12) $C_3F_5^+$ (77)	1.6	1.8	CF_3^+ (9) $C_2F_4^+$ (10) $C_3F_5^+$ (52) $C_4F_7^+$ (29)
	Ne$^+$ ᵇ (21.56)	1.2	1.2	CF^+ (80) CF_2^+ (15) CF_3^+ (1) $C_2F_4^+$ (4)	1.7	1.7	CF^+ (21) CF_3^+ (45) $C_2F_3^+$ (27) $C_3F_4^+$ (4) $C_3F_6^+$ (3)	1.7	1.8	CF_3^+ (31) $C_3F_3^+$ (3) $C_2F_4^+$ (3) $C_3F_4^+$ (7) $C_3F_5^+$ (53) $C_4F_6^+$ (1) $C_4F_8^+$ (2)

ᵃ These polarizabilities (in units of Å$^3 = 10^{-30}$ m^3) have been taken from values obtained in our previous study [9].

ᵇ Ion branching ratios include products resulting from the reactions of cations formed in the flow tube; OH$^+$ (5%) and HeNe$^+$ (3%).

fects. In particular, there are notable differences observed for the unsaturated PFCs between the $\tilde{X}$ and $\tilde{A}$ ionic states (see Fig. 2).

The cation branching ratios obtained from the ion–molecule studies compared to those obtained in our TPEPICO experiments for the PFCs C_2F_6, C_3F_8, n-C_4F_{10}, C_2F_4, C_3F_6, and 2-C_4F_8, are illustrated in Figs. 3–8, respectively. Lines (dashed and continuous) are used to represent the TPEPICO data, and symbols the ion–molecule data. Figs. 1–8 are used in the following discussion to help interpret the ion–PFC reaction processes, and to provide valuable insight into the dynamics of charge transfer. In the following discussion, the thermochemical data used to determine the enthalpy of the reactions presented are taken from the compilation by Lias et al. [28].

4. Discussion

4.1. Reaction rate coefficients

Reactions of CF_4 with N_2^+, Ar$^+$, and F$^+$ are efficient, having within experimental error rate coefficients equal to the collisional values. The reaction with Ne$^+$, by contrast, is inefficient ($\sim$6% of collisional). The TPES of CF_4 is illustrated in Fig. 1(a) (adapted from [29]). Fig. 1(a) shows that at the recombination energies of N_2^+ and Ar$^+$, the $\tilde{X}$ state of CF_4^+ is accessible, and at the recombination energy of F$^+$, the $\tilde{A}$ state of CF_4^+ is reached. However, at the recombination energy of Ne$^+$, which is slightly lower in energy than the threshold of the $\tilde{C}$ ionic state of CF_4, no resonances appear in the spectrum. Therefore,

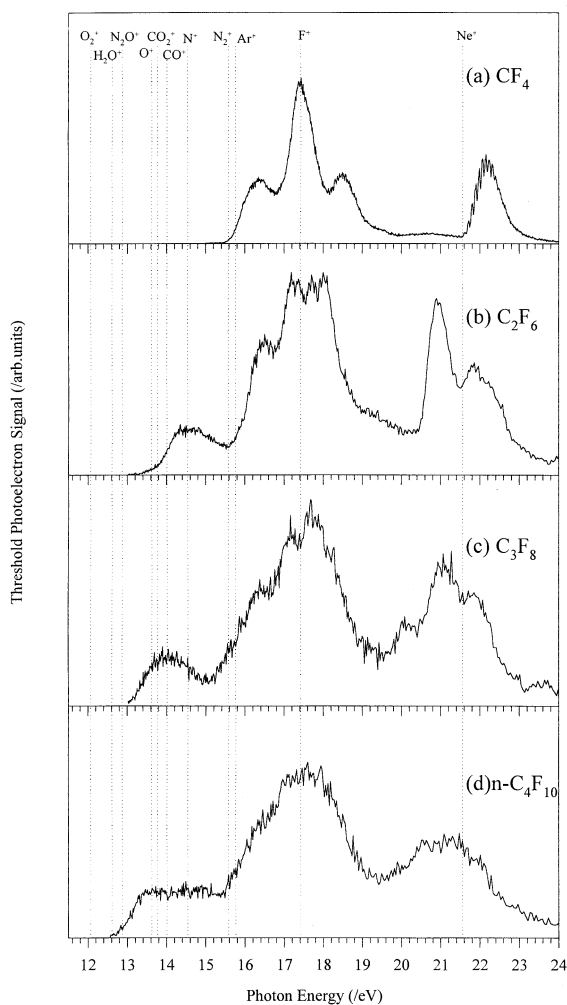Fig. 1. TPES of the saturated PFCs, (a) CF_4, (b) C_2F_6, (c) C_3F_8, and (d) n-C_4F_{10}. The recombination energies of the reagent cations are indicated.

Fig. 2. TPES of the unsaturated PFCs, (a) C_2F_4, (b) C_3F_6, and (c) 2-C_4F_8. The recombination energies of the reagent cations are indicated.

if the reaction of CF_4 with Ne^+ can occur only by long-range charge transfer, the reaction rate coefficient would be expected to be small, as is observed. The reaction of Ne^+ with CF_4 was further investigated at 495 K, and an increase in the rate coefficient (by a factor of 1.6) was observed. The internal energy at 298 K of CF_4 is 0.07 eV (calculated using the molecular vibrational frequencies given by Monostori and Weber [30] and by Maki et al. [31]) whereas at 495 K it is 0.17 eV. This increase in the population of excited vibrational levels of CF_4 may result in a more
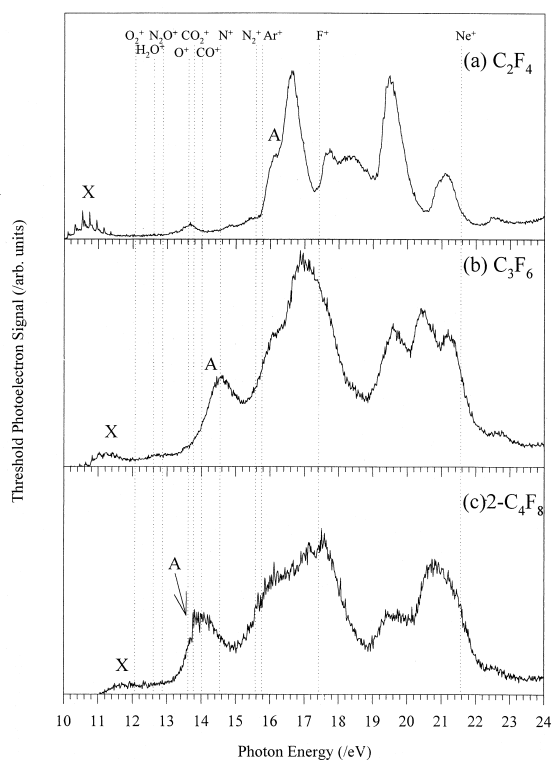
favourable Franck-Condon overlap between the ground electronic state of neutral CF_4 and the $\tilde{C}$ state of CF_4^+, resulting in the observed increase in the measured reaction rate coefficient.

The recombination energies of N_2^+ and Ar^+ are close to the ionisation onset potential of CF_4 [see Fig. 1(a)]. Therefore, there are poor Franck-Condon factors connecting CF_4 to the ground ionic state at these energies. Nevertheless, as mentioned previously, both reactions are efficient with $k_{obs}/k_c \sim 1$. This may suggest that an efficient short-range dissociative charge transfer takes place for the reactions with N_2^+ and Ar^+ [reaction (6)] and significant distortion of the potential energy curves occurs or an intimate reaction complex is formed. An alternative explanation is that as long as there is an energy resonance, the size of the Franck-Condon factor connecting the neutral molecule to an excited molecular ion state is not critical in
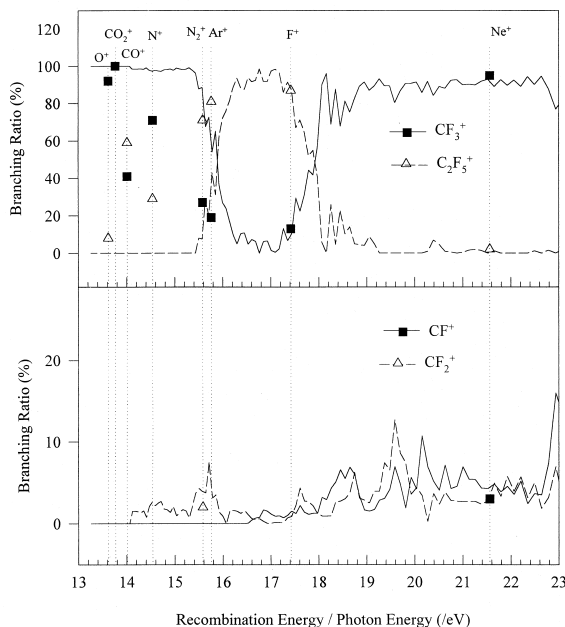
Fig. 3. TPEPICO breakdown diagram for C_2F_6 compared to the cation product branching ratios obtained from the ion–molecule reactions.
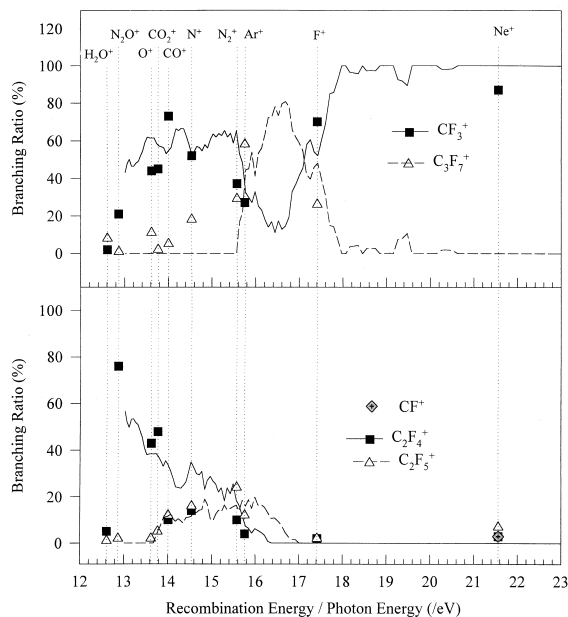

Fig. 4. TPEPICO breakdown diagram for C_3F_8 compared to the cation product branching ratios obtained from the ion–molecule reactions. The product cations $CF_3^+ \cdot H_2O$ (72%) and $C_2F_5^+ \cdot H_2O$ (12%) resulting from the reaction with H_2O^+ are not indicated.

determining the efficiency of a long-range charge-transfer mechanism.

At the recombination energies of many of the reagent cations, the unsaturated PFCs have no photo-electron bands in their PES (C_2F_4 [25], C_3F_6 [26], and 2-C_4F_8 [27]), as is illustrated in the TPES of these molecules shown in Fig. 2(a)–(c). Nevertheless, with the exception of the reactions of N_2O^+ and CO_2^+ with C_2F_4, all of the cation-unsaturated PFC reactions proceed with rate coefficients close to the calculated collisional values. Recently, we have also investigated

$$Kr^+ + C_2F_4 \rightarrow C_2F_4^+ + Kr \qquad (9)$$

For reaction (9) the recombination energy of Kr^+ (14.0 eV) is far removed from any C_2F_4 photoelectron band. Therefore, if long-range charge transfer dominated, we should expect a very small rate coefficient, but this is not observed. The measured rate coefficient, $k_{obs} = 2.8 \times 10^{-10}$ cm^3 molecule^{-1} s^{-1}, is 40% of the collisional, $k_c = 7.1 \times 10^{-10}$ cm^3 molecule^{-1} s^{-1}.

The reactions of the larger saturated PFCs with the

reagent cations, at least for those cations that can exothermically charge transfer with the PFCs, occur with reaction rate coefficients close to the collisional values, although the recombination energy of some of the reagent cations fall in regions with unfavourable Franck-Condon factors [Fig. 1(b)–(d)].

In summary long-range charge transfer, whose reactivity is controlled by Franck-Condon overlap, is not expected to take place for many of the reactions of the cations with the saturated and unsaturated PFCs.

The above-mentioned results beg the question: why do the unsaturated and saturated PFCs react upon nearly every collision with a reagent cation even when near-zero (or zero) Franck-Condon factors are associated with the transition to the ionic state, whilst CF_4 does not? Another way to phrase this question is to ask: why is there no efficient charge transfer from CF_4 to Ne^+ via a short-range process, given that long-range charge transfer is hindered because of poor Franck-Condon overlap? Clearly, there must be a significant barrier to short-range charge transfer for
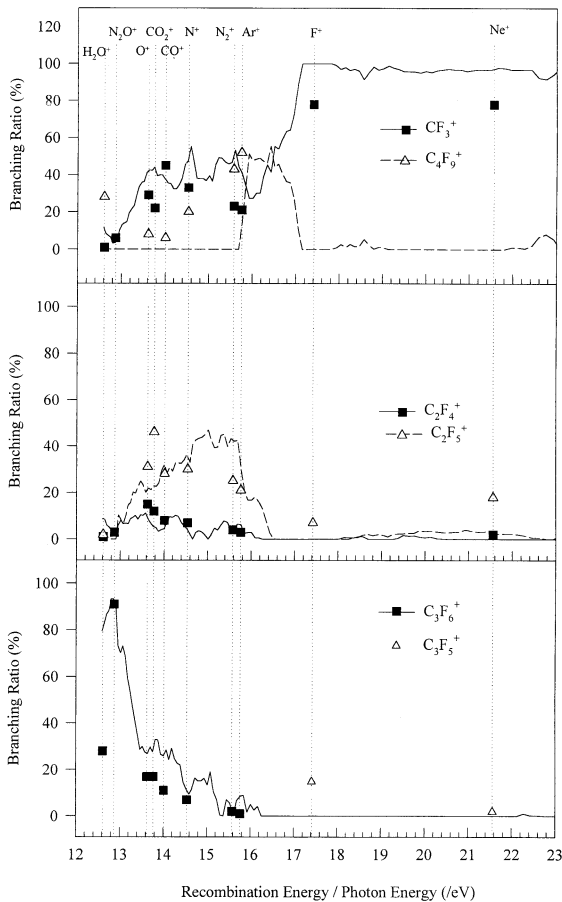
Fig. 5. TPEPICO breakdown diagram for n-C_4F_{10} compared to the cation product branching ratios obtained from the ion–molecule reactions. The product cations $CF_3^+ \cdot H_2O$ (32%) and $C_2F_5^+ \cdot H_2O$ (8%) resulting from the reaction with H_2O^+ and $C_3F_7^+$ (3%) resulting from the reaction with N^+ are not indicated.

this system. To try to understand why this occurs, the dynamics of charge transfer need to be better understood. Toward this goal, we will now compare cation branching ratios obtained from the TPEPICO measurements of the PFCs with those obtained from the SIFT study.

4.2. Ion products: a comparison of SIFT and TPEPICO data to help interpret the mechanisms of charge transfer

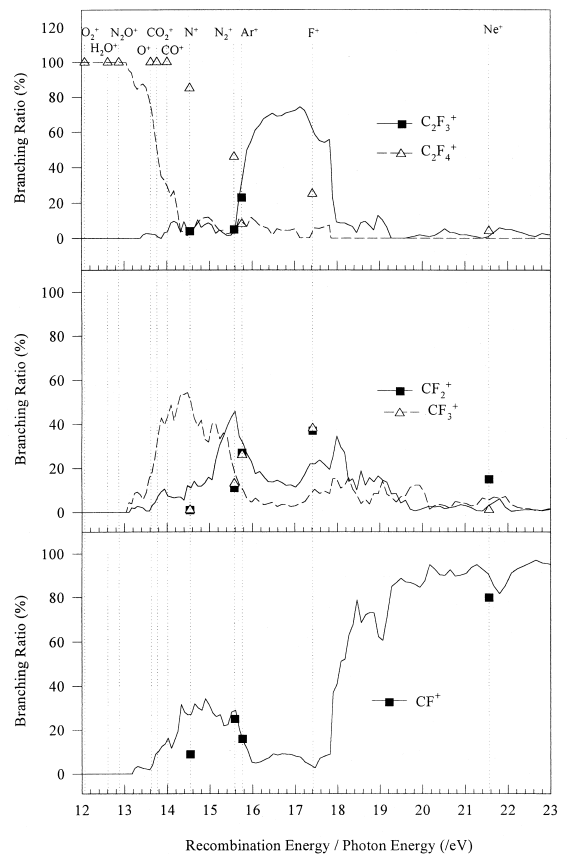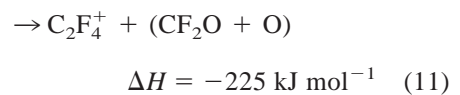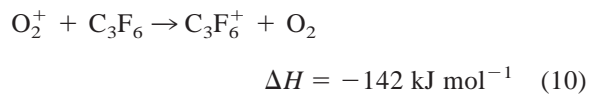In our previous study [9], we observed that for some of the reactions, cation products were observed

Fig. 6. TPEPICO breakdown diagram for C_2F_4 compared to the cation product branching ratios obtained from the ion–molecule reactions.

which could only be explained by a chemical process, i.e. one in which bonds are broken and formed. For such reactions, we argued that charge transfer (nondissociative and dissociative) occurs within an ion–molecule complex, rather than via a long-range mechanism. For example, the reaction of O_2^+ with C_3F_6 results in the product cations $C_2F_4^+$ (13%), $C_3F_5^+$ (10%), and $C_3F_6^+$ (77%). $C_3F_6^+$ results from nondissociative charge-transfer, whereas $C_2F_4^+$ can only result from a chemical reaction:

$$O_2^+ + C_3F_6 \rightarrow C_3F_6^+ + O_2$$

$$\Delta H = -142 \text{ kJ mol}^{-1} \quad (10)$$

$$\rightarrow C_2F_4^+ + (CF_2O + O)$$

$$\Delta H = -225 \text{ kJ mol}^{-1} \quad (11)$$

Fig. 7. TPEPICO breakdown diagram for C_3F_6 compared to the cation product branching ratios obtained from the ion–molecule reactions.
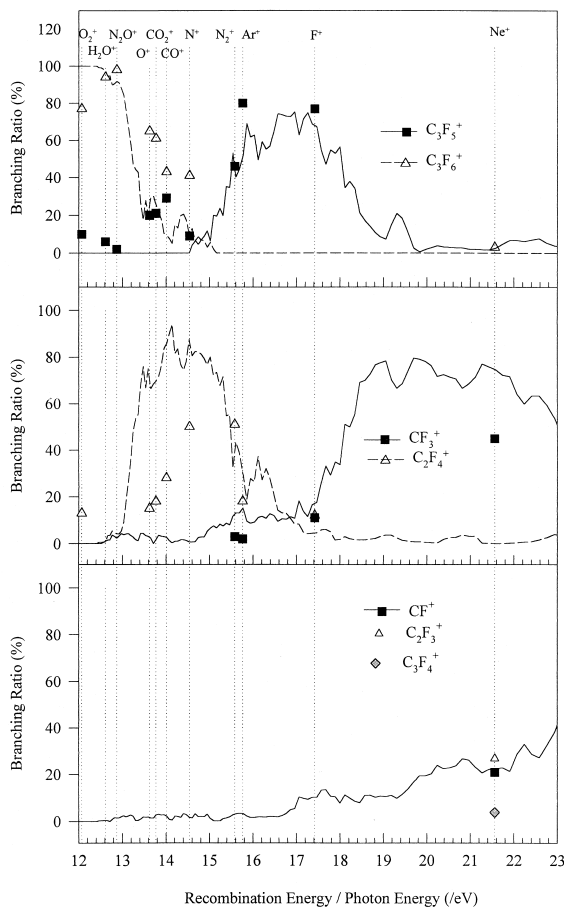

Fig. 8. TPEPICO breakdown diagram for 2-C_4F_8 compared to the cation product branching ratios obtained from the ion–molecule reactions.

The neutral species from the reaction channel resulting in $C_2F_4^+$ cannot be $O_2 + CF_2$ (which would result from dissociative charge transfer) because that route is endothermic ($\Delta H = +71$, 48, and 27 kJ mol^{-1} for the $v = 0$, 1, and 2 vibrational levels of O_2^+, respectively). Similarly, dissociative charge transfer is also endothermic for the production of $C_3F_5^+$, and the reaction must produce FO_2 as the neutral species to make the reaction exothermic. This illustrates that thermodynamically allowed chemical pathways can compete with charge transfer. That a short-range, rather than a long-range, charge transfer occurs is consistent with the recombination energy of O_2^+ lying between the $\tilde{X}$ and $\tilde{A}$ ionic states of C_3F_6 [26], as

illustrated in Fig. 2(b), i.e. in an energy region where the PES shows no resonances. Another example illustrating charge transfer competing with chemical reaction channels, this time from the saturated PFCs, comes from the reactions of O^+, CO^+, and N^+ with C_2F_6; one of the observed cation products, $C_2F_5^+$, is thermodynamically allowed only with FO, FCO, and NF, respectively, being formed as neutral products. For a number of cation–PFC reactions, both chemical and dissociative charge-transfer pathways are exothermic. For such cases, a comparison with the TPEPICO and TPES measurements may be helpful in interpreting the reaction channel(s) involved.

4.3. Saturated PFCs CF_4, C_2F_6, C_3F_8, and n-C_4F_{10}

It is observed that the cation branching ratios obtained from the SIFT measurements follow the general trend obtained in the TPEPICO measurements (Figs. 3–5 for C_2F_6, C_3F_8, and n-C_4F_{10}, respectively). There are, however, differences between the cation branching ratios for certain PFCs that require some explanation.

4.3.1. CF_4

Both the TPEPICO and ion–molecule data show that CF_3^+ is the only cation species produced:

$$M^+ + CF_4 \rightarrow CF_3^+ + F + M \qquad (12)$$

$$h\nu + CF_4 \rightarrow CF_3^+ + F + e^- \qquad (13)$$
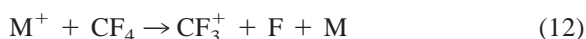
where M = N_2, Ar, F, or Ne, and $h\nu \geq 15.3$ eV. Given that there is only one cation product, no information regarding the (dissociative) charge-transfer mechanism can be inferred from the TPEPICO branching ratio data. We note here that the ground ionic state of CF_4 is dissociative, with $CF_4^+ \rightarrow CF_3^+ + F$. The bound region of the CF_4^+ potential energy surface lies well outside that accessible from the neutral CF_4 ground state. Indeed the CF_4^+ ion has only been observed from electron impact ionisation studies of a supersonic tetrafluoromethane molecular beam, in which CF_4^+ is believed to be stabilised by intermolecular interaction in ionised aggregates [32].

For M = F, the neutral product could be F_2, i.e. F^+ could react with CF_4 by means of a chemical channel rather than dissociative charge transfer:

$$F^+ + CF_4 \rightarrow CF_3^+ + F_2$$
$$\Delta H = -425 \text{ kJ mol}^{-1} \quad (14)$$
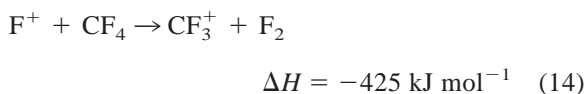
However, there is an intense photoelectron band in the PES of CF_4 at about 17 eV, resulting from the ionisation of a lone-pair fluorine electron. This suggests that (long-range) charge transfer from CF_4 to F^+ takes place and reaction (14) does not occur.

Long-range charge transfer is hindered for the reaction with Ne^+ because of the zero Franck-Condon overlap connecting $\tilde{X}$ CF_4 to $\tilde{C}$ CF_4^+ at the recombi-nation energy of Ne^+. That a short-range process is also inefficient indicates that for any Ne^+–CF_4 complex formed there is still a significant potential energy barrier for the transfer of an electron. It is worthy to note that the electron involved in the resonant charge-transfer to Ne^+ is from a sigma bonding C–F orbital [33]. It is possible that this electron does not significantly feel the influence of the approaching Ne^+ because the electrons associated with the fluorine lone pairs will to some extent shield it. Thus, the potential energy barrier to charge transfer must remain large even for a short-range interaction in which an ion complex is formed. Transfer of an electron from a fluorine lone-pair orbital will be inefficient because of the large energy defect involved.

4.3.2. C_2F_6

Fig. 3 illustrates the cation branching ratios from the TPEPICO experiment with C_2F_6 compared to those obtained from the ion–molecule reactions. The reagent cations O_2^+, H_2O^+, and N_2O^+ do not appear in Fig. 3. For these cations, charge transfer is endothermic (as are reactions involving a complex intermediate leading to products containing atoms from both interacting particles). Charge transfer, however, is energetically possible for all the other reagent cations.

Fig. 3 shows that there are considerable differences in the cation branching ratios obtained from the reactions of O^+, CO^+, and N^+ compared to those obtained from TPEPICO measurements at photon energies equal to the recombination energies of these cations. For photon energies greater than 13.4 eV, but less than 15.6 eV, an electron is ionised from a C–C σ-bonding orbital resulting in the production of only one cation, CF_3^+:

$$h\nu + C_2F_6 \rightarrow CF_3^+ + CF_3 + e^- \qquad (15)$$

In comparison, whilst the reactions with O^+, CO^+, and N^+ do produce CF_3^+ (with branching ratios of 92%, 41%, and 71%, respectively), a substantial cation branching ratio is associated with the only other product cation, $C_2F_5^+$. As mentioned previously, the production of $C_2F_5^+$ by dissociative charge transfer to O^+, CO^+, and N^+ is endothermic:

$$M^+ + C_2F_6 \rightarrow C_2F_5^+ + F + M \qquad (16)$$

$\Delta H = 108$, 69, and 20 kJ mol^{-1} for M = O, CO, and N, respectively. The only exothermic channel is one for which MF is formed. Therefore, a collision complex must be formed. Within this complex electrophilic attack on a C–F bond results in the $C_2F_5^+$ product cation, and electrophilic attack on the C–C bond of the PFC results in the formation of CF_3^+. As can be seen from Fig. 1(b), there are poor Franck-Condon factors connecting C_2F_6 to its ground ionic state at the recombination energies of O^+. However, this does not apply for the reactions with CO^+ and N^+. At the recombination energies of these two cations, there are reasonable Franck-Condon factors connecting neutral C_2F_6 to its $\tilde{X}$ ionic state. According to the Franck-Condon overlap criterion, mentioned at the beginning of this article, only long-range charge transfer should be expected for these reactions. No short-range reaction channels leading, in this case, to $C_2F_5^+$ (and COF or NF) should take place.

A plausible explanation for the observed $C_2F_5^+$ product cation for the reactions with CO^+ and N^+ can be obtained by considering the type of molecular orbital in the neutral species from which the electron is being (resonantly) removed. The $\tilde{X}$ ionic state of C_2F_6 results from the removal of an electron from a C–C bond. For many trajectories, the electron associated with this bond will be shielded from the approaching reagent cation by the surrounding fluorine atoms. For such trajectories, there will be a large potential energy barrier to long-range charge transfer. Charge transfer will thus have a greater probability of occurring once C_2F_6 and CO^+/N^+ form an intimate complex. Within this complex, electrophilic attack on the C–C bond occurs leading to the observed CF_3^+ cation and other (chemical) reaction channels becoming available. In this case, the electrophilic attack by the cation on a fluorine atom results in the production of $C_2F_5^+$ + COF/FN.
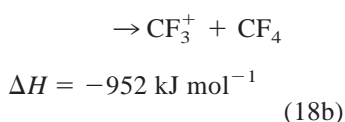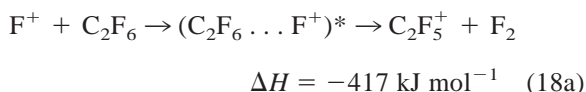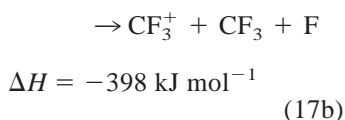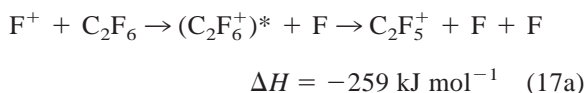
CO_2^+, whose recombination energy lies between that of O^+ and CO^+, may also react with C_2F_6 via a short-range interaction. That there is only one cation product, CF_3^+, implies that electrophilic attack by CO_2^+ on a fluorine atom, leading to $C_2F_5^+$, must be endothermic. This is likely to be the case, given that the CO_2–F bond strength is weak. This example serves to illustrate that only differences between TPEPICO and ion–molecule cation branching ratios can be used to indicate that a short-range mechanism is operative. If the branching ratios are the same, it is difficult to decide from the data alone whether long-range or short-range charge transfer is favoured.

The recombination energies of N_2^+ and Ar^+ are close to the observed threshold of the $C_2F_6^+$ $\tilde{A}$ repulsive ionic state [24] at ~15.4 eV [see Fig. 1(b)]. For photon energies equal to the recombination energies of N_2^+ and Ar^+, the cation branching ratios from the TPEPICO are approximately 80% for CF_3^+, and approximately 20% for $C_2F_5^+$. As mentioned previously, CF_3^+ results from the removal of a C–C σ bonding electron leading to the formation of $\tilde{X}$ $C_2F_6^+$ high up on its repulsive potential surface. $C_2F_5^+$ results from the elimination of an electron from a π level of the fluorine atoms, leading to the $\tilde{A}$ ionic state of C_2F_6 [24]. The TPEPICO cation branching ratios reflect the relative magnitudes of the photoionisation transition probabilities for accessing the $\tilde{X}$ and $\tilde{A}$ ionic states at these photon energies. The cation branching ratios from the SIFT data, on the other hand, for both the N_2^+ and Ar^+ reactions, give approximately 80% for $C_2F_5^+$, and 20% for CF_3^+. There are two possible ways to interpret these results. One is that during the approach of the cation, significant distortion of the C_2F_6 potential energy surfaces occur which in turn modifies the Franck-Condon factors favouring a charge transfer that involves ionisation of C_2F_6 to the $\tilde{A}$ ionic state. Alternatively, one can interpret the differences by considering that energy resonance rather than good Franck-Condon factors is necessary, and that upon the approach of the cation, short-range charge transfer from a π level of the fluorine atoms is readily available, while charge transfer from the C–C orbital will be hindered because of a shielding effect caused by the electrons in the C–F bonds. Either of these descriptions provides a plausible explanation to the favourable production of $C_2F_5^+$ from the reactions of N_2^+ and Ar^+ with C_2F_6.

For the reaction of F^+ with C_2F_6, the cation products $C_2F_5^+$ and CF_3^+ can be formed exothermi-

cally either by dissociative charge-transfer (long-range or short-range) (17) and/or by a chemical reaction (18):

$$F^+ + C_2F_6 \rightarrow (C_2F_6^+)^* + F \rightarrow C_2F_5^+ + F + F$$

$$\Delta H = -259 \text{ kJ mol}^{-1} \quad (17a)$$

$$\rightarrow CF_3^+ + CF_3 + F$$

$$\Delta H = -398 \text{ kJ mol}^{-1}$$
$$(17b)$$

$$F^+ + C_2F_6 \rightarrow (C_2F_6 \dots F^+)^* \rightarrow C_2F_5^+ + F_2$$

$$\Delta H = -417 \text{ kJ mol}^{-1} \quad (18a)$$

$$\rightarrow CF_3^+ + CF_4$$

$$\Delta H = -952 \text{ kJ mol}^{-1}$$
$$(18b)$$

There is an energy resonance for which there are good Franck-Condon factors to an ionic state of C_2F_6 at the recombination energy of F^+ [Fig. 1(b)], and the cation branching ratios obtained are in excellent agreement with those obtained in the TPEPICO experiment. Therefore, the data suggest that a long-range charge transfer occurs. Similarly, very good agreement is observed for the cation branching ratios between TPEPICO and charge-transfer data for Ne^+, and long-range charge transfer is also proposed. In the light of the above-mentioned discussion with charge transfer to N_2^+ and Ar^+, this may suggest that charge transfer to F^+ and Ne^+ from C_2F_6 corresponds to removal of an electron from an orbital that is not shielded from the approaching reagent cation.

4.3.3. C_3F_8

Fig. 4 shows the comparison of the cation branching ratios obtained from TPEPICO and SIFT measurements. Three of the reagent cations, O_2^+, H_2O^+, and N_2O^+, have recombination energies less than the ionisation onset potential of C_3F_8. O_2^+ is found to be unreactive with C_3F_8, whereas H_2O^+ and N_2O^+ efficiently react with C_3F_8 each resulting in a number of cation products. Since charge transfer is endothermic, H_2O^+ and N_2O^+ can only react with C_3F_8 by a short-range intimate chemical interaction [9].

All the other reagent cations in the series can charge-transfer exothermically with C_3F_8. In our earlier article [9], we favoured a collision complex mechanism for forming $C_2F_4^+ + CF_4$ from C_3F_8 via short-range charge transfer, although long-range charge transfer could not be ruled out at the time. For long-range charge transfer to be exothermic, a migration of an F^- must occur before the resulting ionised system $(C_3F_8^+)^*$ dissociates. The highest occupied molecular orbital of C_3F_8 is expected to be associated with a C–C bond [12]. Removal of an electron from this orbital will lead to dissociative ionisation, and the formation of C_2F_5 and CF_3^+. However, the TPEPICO data show that within the time scale of dissociation of $(C_3F_8^+)^*$, intramolecular rearrangement can occur involving F^- migration from C_2F_5 to CF_3^+ forming $C_2F_4^+$ and CF_4. Nevertheless, the SIFT results indicate that such a mechanism is unlikely to occur via a long-range charge-transfer reaction. Rather the data suggest that short-range ion–molecule mechanisms are taking place. For example, the $C_3F_7^+$ product cation formed from the reactions of O^+, CO_2^+, CO^+, and N^+ with C_3F_8 cannot be accounted for by a long-range mechanism [9]. Furthermore, since the electron participating in the charge transfer is being removed from a C–C molecular orbital, it is likely to be shielded from an approaching cation by the fluorine atoms. All this information, taken together, confirms our original assignment that there is a greater probability for an ion–molecule complex to be formed before long-range charge transfer takes place.

The recombination energies of N_2^+ and Ar^+ are close to threshold for ionisation of an electron from a molecular orbital located predominantly on the fluorine atoms, but also lie in the region where access to the $\tilde{X}$ ionic state is possible. Upon reaction with C_3F_8, both ions result in a higher fraction of $C_3F_7^+$ than obtained by TPEPICO. As described for C_2F_6, a plausible explanation is that an ion–molecule complex is formed, within which enhancement of the dissociative ionisation channel from the $\tilde{A}$ ionic state, in this case leading to $C_3F_7^+$, occurs.

For the F^+ and Ne^+ reactions, whilst cation branching ratios show reasonable agreement with the TPEPICO data, there are slight differences between

the two sets of data. The TPES of C_3F_8 shows intense bands at the recombination energies of these cations. For the F^+ reaction, the observation of product cations $C_2F_4^+$ and $C_2F_5^+$, which are not observed in the TPEPICO measurements at the recombination energy of F^+, implies that a short-range interaction takes place. Nothing conclusive can be said about the Ne^+ reaction, because the small differences in the observed cation branching ratios could arise from reactions with the impurity cations for which no allowance has been made in this study.

4.3.4. n-C_4F_{10}

The cation branching ratios for the TPEPICO and SIFT measurements are presented in Fig. 5. Again, as has been found for the other saturated PFCs, there is generally good agreement between the two data sets, with the ion–molecule branching ratios following the general trend of the branching ratios obtained from the photoionisation measurements, although there are obvious differences, which are discussed below.

As found for C_2F_6 and C_3F_8, O_2^+ is unreactive. Charge transfer is endothermic, because the recombination energy of O_2^+ (12.07 eV) is less than the ionisation onset potential of n-C_4F_{10} (~12.6 eV) [12]. Furthermore, no exothermic short-range (chemical) reaction pathways can be available. H_2O^+ reacts with n-C_4F_{10}, via an intimate interaction as is apparent from the observation of the product cations $CF_3^+ \cdot H_2O$ (32%) and $C_2F_5^+ \cdot H_2O$ (8%). This is not surprising given that the recombination energy of H_2O^+ is close to the ionisation onset potential of n-C_4F_{10}. Similarly, the recombination energy of N_2O^+ occurs just above this threshold, and there is a poor Franck-Condon overlap connecting neutral n-C_4F_{10} to its ground ionic state at the recombination energy of this cation. This may result in a low probability for long-range charge transfer. Although the product cations resulting from the reaction with N_2O^+ are in excellent agreement with those obtained by TPEPICO, short-range dissociative charge transfer may also result in similar product cation branching ratios.

Dissociative charge transfer leading to the observed $C_4F_9^+$ product cation from the reactions with

O^+, CO^+, and N^+ [9], with branching ratios of 8%, 6%, and 20%, respectively, is endothermic. Therefore, the production of this cation requires a chemical reaction in which the reagent cations are included in the neutral product(s). No $C_4F_9^+$ product cation is observed for the reaction with CO_2^+. That no $C_4F_9^+$ product cation is observed for the reaction with CO_2^+ may again illustrate that the CO_2–F bond is weak so that the reaction is likely to be endothermic. Whilst the TPES [Fig. 1(d)] indicates that there are seemingly good Franck-Condon factors for ionisation from neutral n-C_4F_{10} to $\tilde{X}$ n-$C_4F_{10}^+$ at photon energies equal to the recombination energies of O^+, CO_2^+, CO^+, and N^+, the molecular orbital from which an electron is removed is considered to be a C–C σ-bonding orbital [12]. The electron within this orbital may not significantly feel the presence of the reagent cation until an ion–molecule complex is formed. Therefore long-range charge transfer is likely to be inhibited for most approaches of a reagent cation, thus providing an explanation for the observed "short-range" cation products.

Dissociative charge transfer to N_2^+ and Ar^+ resulting in the observed product cation $C_4F_9^+$ is exothermic. However, the differences between the TPEPICO and SIFT cation branching ratios indicate that these cations are reacting with n-C_4F_{10} by a short-range process. Certainly, the recombination energies of these two cations lie in a region of the TPES that marks the end of the ground ionic state and the onset of the first excited ionic state [Fig. 1(d)]. As discussed for C_2F_6 and C_3F_8, the enhancement of the cation branching ratio associated with the $C_4F_9^+$ product cation, compared to the TPEPICO cation branching ratio, implies that an electron is more easily transferred to the reagent cation from a molecular orbital associated with the fluorine atoms, rather than from a (shielded) C–C bond within the ion–molecule complex.

That sizeable branching ratios are associated with the cation products $C_3F_5^+$ (15%) and $C_2F_5^+$ (18%) for the F^+ and Ne^+ reactions, respectively, which are not observed in the TPEPICO data at the recombination energies of these cations, is again indicative of a short-range interaction. The TPES of n-C_4F_{10} shows

reasonably intense resonances at the recombination energies of F^+ and Ne^+. That a short-range interaction is indicated from the cation branching data may imply that charge transfer involves the removal of an electron from a shielded molecular orbital, and hence long-range charge transfer is inhibited.

4.4. Unsaturated PFCs C_2F_4, C_3F_6, and $2\text{-}C_4F_8$

For the saturated PFCs it is observed that the cation branching ratios obtained from the SIFT study in general follow those obtained from the TPEPICO measurements. However, agreement between the cation branching ratios obtained in the TPEPICO and ion–molecule experiments for the unsaturated PFCs (C_2F_4, C_3F_6, and $2\text{-}C_4F_8$) is noticeably poorer compared to the saturated systems, as is illustrated in Figs. 6–8.

4.4.1. C_2F_4

The ionisation of C_2F_4 to produce $C_2F_4^+$ by photons or nondissociative charge transfer is illustrated in Fig. 6. For the ion–molecule reactions, $C_2F_4^+$ is the only product cation for reactions with O_2^+, H_2O^+, N_2O^+, O^+, CO_2^+, and CO^+, and is the dominant product cation for reactions with N^+ and N_2^+:

$$M^+ + C_2F_4 \rightarrow C_2F_4^+ + M \qquad (19)$$

The cation branching ratio for $C_2F_4^+$ for reactions with cations whose recombination energies are greater than 14 eV decreases with increasing recombination energy, dropping to 85% for the reaction with N^+, down to 46% for the reaction with N_2^+, and then decreasing dramatically down to 4% for the reaction with Ar^+. The branching ratio for $C_2F_4^+$ subsequently increases to 22% for the F^+ reaction. In comparison, the photoionisation studies show that the branching ratio of $C_2F_4^+$ has essentially fallen away to zero by ~ 14.4 eV. The recombination energy for any of the cations mentioned previously, with the exception of Ar^+, falls in a region of the PES of C_2F_4 absent of any resonant bands. This, taken together with the marked differences in the cation branching ratios between the TPEPICO and SIFT measurements, confirms our original conclusion [9] that charge transfer occurs via a short-range interaction with O_2^+, H_2O^+, N_2O^+, O^+, CO_2^+, CO^+, N^+, N_2^+ ($v = 0$), and F^+. This means that exothermic chemical pathways can compete with charge-transfer (dissociative and nondissociative). Certainly one of the cation products observed from the reaction with N^+, $C_2F_3^+$, with a branching ratio of 4%, can only be formed if a fluorine atom bonds with N.

The recombination energy of Ar^+ lies just above the threshold of the $\tilde{A}$ ionic state of C_2F_4 [see Fig. 2(a)]. At this energy poor Franck-Condon factors apply. That the cation branching ratios observed agree well with those obtained by TPEPICO, may imply that the Franck-Condon factors are sufficient for a long-range charge transfer to occur, with the electron being removed from an unshielded orbital.

The recombination energy for N_2^+ ($v = 0$) is just 0.18 eV less than that of Ar^+. Yet this is sufficient to ensure that the $\tilde{A}$ ionic state of C_2F_4 cannot be accessed. An ion–molecule complex must be formed, within which chemical pathways are accessible and significant distortion of the potential energy surfaces can result. This explains the marked differences observed in the cation branching ratios observed between those obtained for the Ar^+ and N_2^+ reactions. However, we know that a significant fraction ($\sim 40\%$) of our N_2^+ cations are formed vibrationally excited with $v = 1$ [9]. That short-range reactions within an ion–molecule complex still dominate for these vibrationally excited cations may be explained by the observation that there are only small Franck-Condon factors connecting N_2^+ ($v = 1$) to N_2 ($v = 0$). This may inhibit dissociative charge-transfer from C_2F_4 leading to $C_2F_3^+ + F$ occurring outside of an ion–molecule complex.

Ne^+ reacts with C_2F_4 at the collisional rate, with cation branching ratios similar to those obtained in the TPEPICO measurements at a corresponding photon energy equal to 21.6 eV, the recombination energy of Ne^+. This may indicate that a purely long-range charge transfer process is taking place.

4.4.2. C_3F_6

The TPEPICO and SIFT data for C_3F_6 are illustrated in Fig. 7. Significant differences in the cation

branching ratios exist between the TPEPICO and ion–molecule data for the reactions with O_2^+, H_2O^+, N_2O^+, O^+, CO_2^+, CO^+, and N^+ (for which nondissociative charge transfer is a major reaction channel). These differences indicate that a short-range mechanism operates for reactions with these cations. In agreement with this suggestion, the recombination energies of O_2^+, H_2O^+, N_2O^+, O^+, CO_2^+, and CO^+ lie within a region of the PES of C_3F_6 devoid of any resonances [26]. Evidence for a short-range interaction also comes from the cation products observed following reaction with O_2^+. For example, one product cation is $C_2F_4^+$ with a branching ratio of 13%. Formation of this cation by dissociative charge transfer:

$$O_2^+ + C_3F_6 \rightarrow C_2F_4^+ + CF_2 + O_2 \qquad (20)$$

is endothermic by 71, 48, and 27 kJ mol^{-1} for the $v = 0$, 1, and 2 vibrational levels of O_2^+, respectively. Dissociative charge-transfer to produce another observed product cation, $C_3F_5^+$ (with a branching ratio of 10%), is also endothermic for reaction with O_2^+ ($v = 0$, 1, and 2). Indeed the production of $C_3F_5^+$ is endothermic by dissociative charge transfer if the recombination energy of the reagent cation is less than 13.8 eV. Yet, in addition to the reaction with O_2^+, $C_3F_5^+$ is an observed product cation for reaction with H_2O^+ (recombination energy = 12.61 eV), N_2O^+ (recombination energy = 12.87 eV) and O^+ (recombination energy = 13.62 eV), with branching ratios of 6%, 2%, and 20%, respectively.

At the recombination energy of N^+, good Franck-Condon factors connect the ground state of C_3F_6 to its first excited ionic state, as is illustrated in Fig. 2(b). This suggests that long-range charge transfer should occur. Why, therefore, are significantly different cation branching ratios obtained from the TPEPICO and SIFT measurements? A plausible explanation, and used in the interpretation of the reactions with the saturated PFCs, is that the electron involved in the charge transfer is being removed from an orbital which is shielded from the approaching reagent cation by the fluorine atoms, i.e. there is a potential energy barrier to long-range charge transfer for many cation-PFC trajectories. To overcome this barrier, a short-range interaction is necessary, and then energy resonance and curve crossing are unimportant. This assignment is supported by conclusions drawn from the TPEPICO data [13] where there is a strong suggestion that the electron is ionised from a molecular orbital associated with the C–C bond.

For N_2^+, Ar^+, and F^+, good agreement is observed between the TPEPICO and ion–molecule data. At photon energies corresponding to the recombination energies of N_2^+ and Ar^+, the major product cations are $C_2F_4^+$ and $C_3F_5^+$, and at a photon energy equal to the recombination energy of F^+, $C_3F_5^+$ is the major product cation. This agrees well with the results from the ion–molecule study. At energies corresponding to the recombination energies of N_2^+, Ar^+, and F^+, there are good Franck-Condon factors connecting the ground state of the neutral molecule to one of its ionic states. It should also be noted that the electron transferred to these three cations is thought to originate from an outermost molecular orbital associated with the fluorine atoms [13], and therefore any shielding of the electron from the approaching cation should be small. Thus, the data suggest that a long-range charge-transfer mechanism dominates.

At the recombination energy of Ne^+, no PES is available. However, our TPES data show a reasonably intense resonance at the recombination energy of Ne^+. This, together with the observation that the cation branching ratios obtained from the ion–molecule reaction are in good agreement with those obtained by TPEPICO, may imply that long-range charge transfer occurs, with the electron being transferred from an unshielded molecular orbital.

4.4.3. 2-C_4F_8

Fig. 8 shows the comparison between the TPEPICO and ion–molecule cation branching ratio data. Nondissociative charge-transfer is the dominant mechanism for the reactions of 2-C_4F_8 with O_2^+, H_2O^+, N_2O^+, O^+, and N^+ reactions, and is a major mechanism for the CO_2^+ and CO^+ reactions, with branching ratios of 91%, 85%, 99%, 53%, 20%, 8%, and 73% for M = O_2, H_2O, N_2O, O, CO_2, CO, and N, respectively. N_2^+ reacts with 2-C_4F_8 by means of dissociative ionisation channels only.

Although there is reasonable agreement in the branching ratios obtained for the reaction of O_2^+ and the TPEPICO data, at the recombination energy of this cation, one of the cation products observed in the ion–molecule data, $C_3F_5^+$ (with a branching ratio of 5%), cannot be produced from dissociative charge transfer:

$$O_2^+ + 2\text{-}C_4F_8 \rightarrow C_3F_5^+ + CF_3 + O_2$$

$$\Delta H \geq 59 \text{ kJ mol}^{-1} \quad (21)$$
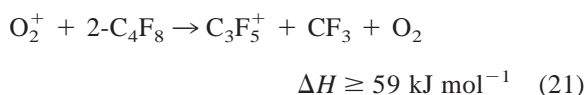
This implies that short-range charge transfer is occurring for the reactions of O_2^+ with $2\text{-}C_4F_8$:

$$O_2^+ + 2\text{-}C_4F_8 \rightarrow C_3F_5^+ + (CF_3O_2) \quad (22)$$
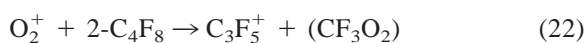
The reaction with N_2O^+ is interesting in that little dissociative ionisation occurs (1%) although its recombination energy is greater than those of O_2^+ and H_2O^+, both of which react with $2\text{-}C_4F_8$ to produce a number of dissociative cation products. Instead, non-dissociative charge transfer dominates:

$$N_2O^+ + 2\text{-}C_4F_8 \rightarrow C_3F_5^+ + CF_3 + N_2O \quad (1\%)$$
$$(23)$$

$$\rightarrow C_4F_8^+ + N_2O \quad (99\%) \quad (24)$$
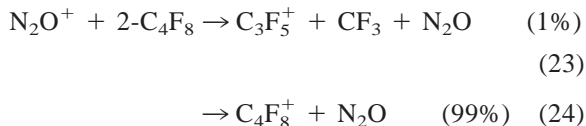
In comparison, the TPEPICO data show that $C_3F_5^+$ accounts for approximately 20% of the cation products at the photon energy corresponding to the recombination energy of N_2O^+. Thus, a short-range $N_2O^+ \ldots 2\text{-}C_4F_8$ interaction is indicated.

The PES of $2\text{-}C_4F_8$ shows a Franck-Condon minimum at the recombination energies of H_2O^+ and N_2O^+, and therefore this agrees with the short-range mechanism proposed previously. What does not agree with this proposal, is that at the recombination energy of O_2^+ good Franck-Condon factors are available to connect the ground electronic state of $2\text{-}C_4F_8$ to its ground ionic state. However, the ground ionic state of $2\text{-}C_4F_8$ is considered to arise as a result of an electron removed from the π component of the C=C double bond [13]. Hence, although there are good Franck-Condon factors, long-range charge transfer may be hindered because of a Coulombic barrier resulting from the surrounding fluorine atoms, shielding the electron in this double bond from the presence of the approaching reagent cation.

There are also good Franck-Condon factors connecting $2\text{-}C_4F_8$ to its $\tilde{A}$ ionic state at the recombination energies of O^+, CO_2^+, CO^+, and N^+. Nevertheless, there are significant differences in the cation branching ratios between the TPEPICO and SIFT data, indicating that a short-range process is taking place for the reactions of these cations with $2\text{-}C_4F_8$. This agrees with our assignment of the second PES band of $2\text{-}C_4F_8$ to be originating from an electron ionised from a C–C bond [13].

There is good agreement between the TPEPICO and SIFT product cation branching ratios for the reactions with N_2^+ and Ar^+, indicating that long-range charge transfer dominates for these reactions. That there are intense resonances observed in the PES of $2\text{-}C_4F_8$ at the recombination energies of these cations agrees with this proposal, providing this structure results from the removal of an electron from a molecular orbital which is not shielded from an approaching reagent cation.

There are differences between the TPEPICO and SIFT cation branching ratios at the recombination energies corresponding to the reactions of F^+ and Ne^+ with $2\text{-}C_4F_8$. This indicates a short-range reaction process. However, the PES of $2\text{-}C_4F_8$ shows an intense band peaking close to the recombination energy of F^+, and the TPES shows intense structure at the recombination energy of Ne^+. The proposed short-range mechanism is therefore only valid if the electron to be removed from $2\text{-}C_4F_8$ is in a molecular orbital shielded from the approaching reagent cation.

5. Conclusions

The interpretation of the reactions of a large number of atomic and molecular cations with several small saturated and unsaturated PFCs in terms of photoionisation (PES, TPES, and TPEPICO) data, provides a valuable insight into charge-transfer processes. From this study, some important conclusions regarding the dynamics of the charge-transfer process have been obtained. Further studies are required to

verify the general applicability of these conclusions. We describe a long-range charge-transfer process as one in which there is little or no distortion of the potential energy surfaces involved in the reaction. The salient points may be summarised as follows. For cation reactions with the PFCs, long-range charge transfer has a high probability of occurring when the following criteria are met:

(1) there is an energy resonance connecting the neutral molecule to an ionic state at the recombination energy of the reagent cation, i.e. Franck-Condon factors do not seem to be significant in determining the efficiency of a long-range charge transfer and

(2) the electron that is involved in the charge transfer is removed from a molecular orbital that is not shielded from the approaching reagent cation by other molecular orbitals of the reactant molecule.

If the electron involved in a charge-transfer reaction is originally in a molecular orbital shielded from the approaching cation, then even if good Franck-Condon factors connect the electronic state of the neutral molecule to an ionic state, the potential energy barrier to long-range charge transfer will be significantly larger than for an electron being transferred from an unshielded orbital. The cation will then have a greater probability of reacting with the neutral PFC molecule via a short-range mechanism, so that, if an ion–molecule complex is formed, charge transfer may be competing with exothermically allowed chemical reaction channels in which bonds are broken and formed. Differences in the cation branching ratios between those obtained by the TPEPICO and SIFT experiments will result if any chemical pathways are involved. In such a scenario, there is a possibility that for some approaches of the reagent cation an electron may still be transferred at large cation–PFC distance providing the trajectory is such that shielding of the electron orbital by the fluorine atoms is minimised. Otherwise, on more hindered approaches, the cation undergoes a more intimate interaction with the reactant neutral molecule. Such a competition between these processes would lead to the differences between the observed TPEPICO and ion–molecule branching ratios.

The aim of this study, to obtain a better understanding of the dynamics of charge-transfer processes, has been achieved. We hope this and other studies will help with the development and improvement of models used to predict the optimal conditions for industrial plasma processes, such as the etching of microcircuit chips. Finally, we comment that electron transfer reactions of molecular anions are expected to be subject to similar dynamical constraints arising from geometry changes. This is confirmed by the study of Grimsrud et al. on some reactions of SF_6^- [34].

References

[1] M.T. Bowers, D.D. Elleman, Chem. Phys. Lett. 16 (1972) 486.

[2] J. Gauglhofer, L. Kevan, Chem. Phys. Lett. 16 (1972) 492.

[3] M.T. Bowers, T. Su, Adv. Electron. Electron. Phys. 34 (1973) 223.

[4] J.B. Laudenslager, W.T. Huntress Jr., M.T. Bowers, J. Chem. Phys. 61 (1974) 4600.

[5] J.D. Kelley, G.H. Bearman, H.H. Harris, J.J. Leventhal, Chem. Phys. Lett. 50 (1977) 295.

[6] R.J. Shul, R. Passarella, B.L. Upschulte, R.G. Keesee, A.W. Castleman Jr., J. Chem. Phys. 86 (1987) 4446.

[7] R.J. Shul, B.L. Upschulte, R. Passarella, R.G. Keesee, A.W. Castleman Jr., J. Phys. Chem. 91 (1987) 2556.

[8] C.A. Mayhew, J. Phys. B: At. Mol. Opt. Phys. 25 (1992) 1865.

[9] G.K. Jarvis, C.A. Mayhew, R.P. Tuckett, J. Phys. Chem. 100 (1996) 17166.

[10] C.A. Mayhew, D. Smith, J. Phys. B: At. Mol. Opt. Phys. 23 (1990) 3139.

[11] T.L. Williams, L.M. Babcock, N.G. Adams, Int. J. Mass Spectrom. 185/186/187 (1999) 759.

[12] G.K. Jarvis, K.J. Boyle, C.A. Mayhew, R.P. Tuckett, J. Phys. Chem. A 102 (1998) 329.

[13] G.K. Jarvis, K.J. Boyle, C.A. Mayhew, R.P. Tuckett, J. Phys. Chem. A 102 (1998) 3230.

[14] M. Chau, M.T. Bowers, Int. J. Mass Spectrom. Ion. Phys. 24 (1977) 191.

[15] R. Richter, W. Lindinger, in *Proceedings from the Symposium on Atomic and Surface Physics* (Inst. Atomphysik, Innsbruck, 1986), p. 203.

[16] D. Smith, N.G. Adams, E. Alge, J. Phys. B. 17 (1984) 461.

[17] R.A. Morris, J.M. Van Doren, A.A. Viggiano, J.F. Paulson, J. Chem. Phys. 97 (1992) 173.

[18] D.M. Smith, R.P. Tuckett, K. Yoxall, K. Codling, P.A. Hatherly, J.F.M. Aarts, M. Stankiewicz, J. Chem. Phys. 101 (1994) 10559.

[19] P.A. Hatherly, D.M. Smith, R.P. Tuckett, Z. Phys. Chem. (Munich) 195 (1996) 97.

[20] D. Smith, N.G. Adams, Adv. At. Mol. Phys. 24 (1988) 1.

[21] N.G. Adams, D. Smith, Int. J. Mass Spectrom. Ion Phys. 21 (1976) 349.

[22] G. Gioumousis, D.P. Stevenson, J. Chem. Phys. 29 (1958) 294.

[23] C.R. Brundle, M.B. Robin, H. Basch, J. Chem. Phys. 53 (1970) 2196.

[24] I.G. Simm, C.J. Dandy, J.H.D. Eland, Int. J. Mass Spectrom. Ion Phys. 14 (1974) 285.

[25] J.A. Sell, A. Kuppermann, J. Chem. Phys. 71 (1979) 4703.

[26] B.S. Freiser, J.L. Beauchamp, J. Am. Chem. Soc. 96 (1974) 6260.

[27] M.B. Robin, G.N. Taylor, N.A. Kuebler, J. Org. Chem. 38 (1973) 1049.

[28] S.J. Lias, J.E. Bartmess, J.F. Liebman, J.L. Holmes, R.D. Levin, W.G. Mallard, J. Phys. Chem. Ref. Data, 1 (1988) 17 (suppl.).

[29] J.C. Creasey, P.A. Hatherly, H.M. Jones, K. Codling, D.M. Smith, I. Powis, R.P. Tuckett, Chem. Phys. 174 (1993) 441.

[30] B. Monostori, A. Weber, J. Chem. Phys. 33 (1960) 1867.

[31] A. Maki, E.K. Plyer, R. Thibault, J. Chem. Phys. 37 (1962) 1899.

[32] G. Hagenow, W. Denzer, B. Brutschy, H. Baumgärtel, J. Phys. Chem. 92 (1988) 6487.

[33] R.N. Dixon, R.P. Tuckett, Chem. Phys. Lett. 140 (1987) 553.

[34] E.P. Grimsrud, S. Chowdhury, P. Kebarle, J. Chem. Phys. 83 (1985) 1059.